JACC: BASIC TO TRANSLATIONAL SCIENCE VOL. 6, NO. 2, 2021

PRECLINICAL RESEARCH

Acute Kidney Injury Results in Long-Term Diastolic Dysfunction That Is Prevented by Histone Deacetylase Inhibition

Danielle E. Soranno, MD,[a,b,c,d] Lara Kirkbride-Romeo, BS,[a] Sara A. Wennersten, BS,[c,e] Kathy Ding,[a] Maria A. Cavasin, PhD,[c,e] Peter Baker, MD,[f] Christopher Altmann, BA,[b] Rushita A. Bagchi, PhD,[c,e] Korey R. Haefner, MS,[c,e] Christian Steinkühler, PhD,[g] John R. Montford, MD,[b,h] Brysen Keith, MS,[d] Katja M. Gist, DO,[i] Timothy A. McKinsey, PhD,[c,e] Sarah Faubel, MD[b]

VISUAL ABSTRACT

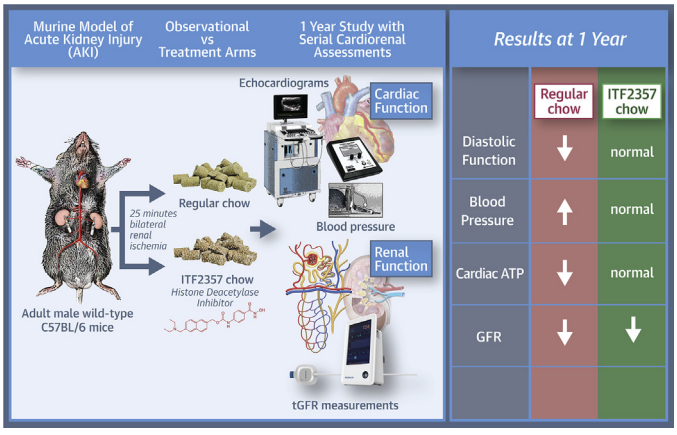

Soranno, D.E. et al. J Am Coll Cardiol Basic Trans Science. 2021;6(2):119–33.

HIGHLIGHTS

- **This is the first long-term (1-year) study to evaluate both the kidney and systemic sequelae of acute kidney injury in mice.**
- **Serial kidney function was measured via transcutaneous glomerular filtration rate.**
- **AKI resulted in diastolic dysfunction, followed by hypertension. Ejection fraction was preserved. One year after AKI, cardiac ATP levels were reduced compared with sham controls.**
- **Mice treated with the histone deacetylase inhibitor, ITF2357, maintained normal diastolic function normal blood pressure, and normal cardiac ATP after AKI.**
- **Metabolomics data suggest that treatment with ITF2357 preserves pathways related to energy metabolism.**

From the [a]Department of Pediatrics, Pediatric Nephrology, University of Colorado, Aurora, Colorado, USA; [b]Department of Medicine, Division of Renal Disease and Hypertension, University of Colorado, Aurora, Colorado, USA; [c]Consortium for Fibrosis Research & Translation, University of Colorado Anschutz Medical Campus, Aurora, Colorado, USA; [d]Department of Bioengineering, University of Colorado Anschutz Medical Campus, Aurora, Colorado, USA; [e]Department of Medicine, Division of Cardiology, University of Colorado, Aurora, Colorado, USA; [f]Department of Pediatrics, Clinical Genetics and Metabolism, University of Colorado, Aurora, Colorado, USA; [g]Italfarmaco, Milan, Italy; [h]Rocky Mountain Regional Veterans Affairs Medical Center, Aurora, Colorado, USA; and the [i]Department of Pediatrics, Pediatric Cardiology, University of Colorado, Aurora, Colorado, USA.
The authors attest they are in compliance with human studies committees and animal welfare regulations of the authors' institutions and Food and Drug Administration guidelines, including patient consent where appropriate. For more information, visit the Author Center.

Manuscript received May 21, 2020; revised manuscript received November 19, 2020, accepted November 19, 2020.

ISSN 2452-302X https://doi.org/10.1016/j.jacbts.2020.11.013

ABBREVIATIONS AND ACRONYMS

AKI = acute kidney injury

ATP = adenosine triphosphate

BUN = blood urea nitrogen

HDACi = histone deacetylase inhibitor

MAP = mean arterial pressure

PSR = picrosirius red

SCr = serum creatinine

tGFR = transcutaneous glomerular filtration rate

SUMMARY

Growing epidemiological data demonstrate that acute kidney injury (AKI) is associated with long-term cardiovascular morbidity and mortality. Here, the authors present a 1-year study of cardiorenal outcomes following bilateral ischemia-reperfusion injury in male mice. These data suggest that AKI causes long-term dysfunction in the cardiac metabolome, which is associated with diastolic dysfunction and hypertension. Mice treated with the histone deacetylase inhibitor, ITF2357, had preservation of cardiac function and remained normotensive throughout the study. ITF2357 did not protect against the development of kidney fibrosis after AKI.

Acute kidney injury (AKI) is common in both pediatric and adult hospitalized patients (1,2). Patients who develop AKI have worse outcomes than those who do not, including increased morbidity and mortality, increased hospital length of stay, and increased costs of hospitalization (3–7). AKI causes nonrenal organ dysfunction, and the leading cause of death of patients with AKI is systemic diseases, rather than AKI itself (8–10). Murine models have demonstrated the short-term systemic effects of AKI, including an increase in serum interleukin (IL)-6, lung inflammation, cardiac dysfunction, liver injury, and metabolic perturbances (11–14). These studies have focused on the short-term nonrenal sequelae, typically evaluating outcomes after 24 h to 72 h (15,16). To date, the long-term systemic sequelae of AKI have not been assessed in murine models.

The study of the long-term systemic sequelae of AKI in murine models is warranted because patients who survive their episodes of AKI have increased risks of developing numerous complications in the long term, including cardiovascular disease (17,18). A wealth of data has accumulated demonstrating that patients with AKI have increased risk of heart failure (19–23). Cho et al. recently reported an association between AKI and diastolic dysfunction in elderly patients presenting with femoral neck fracture (24). There is a paucity of literature investigating the pathophysiology linking AKI and long-term risk of heart failure.

Histone deacetylase inhibitors (HDACi) affect epigenetic regulation of gene expression and nongenomic cellular functions (25–27). We have previously demonstrated that ITF2357/givinostat, an HDACi that is currently in phase 3 clinical testing in patients with Duchenne muscular dystrophy, improves diastolic function in a rat model of hypertension and protects against aging-induced diastolic dysfunction in mice (28).

Herein, we performed a 1-year study using our murine model of bilateral ischemia reperfusion AKI to describe the systemic sequelae of 1 episode of AKI on the lung, liver, and heart as well as to assess circulating cytokines, metabolites, and kidney recovery and function. Furthermore, we determined the effect(s) of treatment with HDACi on cardiorenal outcomes including blood pressure, cardiac function, and metabolism. We hypothesized that AKI would lead to long-term systemic sequelae and that HDAC inhibition would improve cardiorenal outcomes.

METHODS

ANIMALS. Experiments were conducted with adherence to the National Institutes of Health Guide for the Care and Use of Laboratory Animals. The protocol was approved by the Animal Care and Use Committee of the University of Colorado, Denver, Colorado. Six- to 7-week-old male C57BL/6 mice (Jackson Laboratories, Bar Harbor, Maine) maintained on a standard diet, and water ad lib. Mice in the ITF2357 treatment group were started on chow on post-operative day 3. ITF2357 chow (Dyets Inc., Bethlehem, Pennsylvania) was custom manufactured by using Teklad 2920X Rodent Diet (Envigo, Indianapolis, Indiana) with 555 mg/kg of ITF2357, providing an approximate dose of 50 mg/kg/day. Twelve-month study controls were aged at Jackson Laboratories and arrived 2 weeks before sacrifice.

GLOMERULAR FILTRATION RATE. Transcutaneous filtration rate (tGFR) measurements were taken using a transdermal continuous renal function monitor (MediBeacon GMBH, Mannheim, Germany) and fluorescein isothiocyanate (FITC) tail-vein injection per manufacturer instructions. Mice were allowed at least 3 days' recovery after baseline readings before surgeries were performed.

SURGERIES. Surgical procedures were performed on 8-week-old mice. Mice were randomized to either

FIGURE 1 Study Schematic

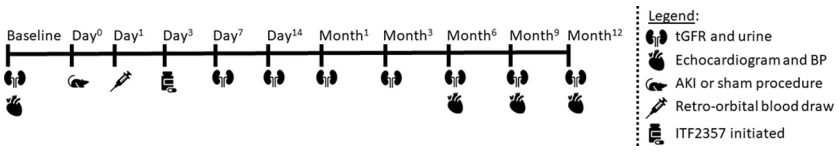

Baseline tGFR and echocardiograms were obtained. Mice were randomized to AKI or sham cohorts on day 0. Male mice underwent 25 min of bilateral renal ischemia or sham procedure. Blood was collected retro-orbitally on day 1 to assess post-operative BUN and SCr, and mice in the AKI cohorts that did not meet inclusion criteria were sacrificed. In the serial study, mice were sacrificed 1, 3, 7, 14 days, 1, 3, 6, 9 and 12 months after the sham or AKI procedure. In the histone deacetylase inhibitor (HDACi) study arm, mice were started on chow containing ITF2357 on post-operative day 3 and maintained on treatment throughout the study; mice were sacrificed at 12 months and tissue was collected for analysis. AKI = acute kidney injury; BP = blood pressure; BUN = blood urea nitrogen; SCr = serum creatinine; tGFR = transcutaneous glomerular filtration rate.

sham or AKI. For all procedures, mice were anesthetized with Ketamine (VetOne, MWI, Boise, Idaho) and Xylazine (VetOne, Bimed-MTC Animal Health Inc., Cambridge, Ontario, Canada). Mice were placed on a heating pad maintained at 36° C to 40°C for the entire procedure. Both renal pedicles were clamped for 25 min via a ventral approach as previously described (12), with the abdomen closed in 2 layers. Post-operatively, mice were administered 750 μl warmed saline/buprenorphine hydrochloride (0.3 mg/ml, PAR Pharmaceuticals, Chestnut Ridge, New York) subcutaneously; 750 μl of normal saline was administered subcutaneously for 5 days.

TISSUE. At 24 h, 100 μl of blood was collected via retro-orbital bleed to determine inclusion status. Criteria for study inclusion in the AKI groups were blood urea nitrogen (BUN) >70 mg/dl or serum creatinine (SCr) >0.7 mg/dl. Thereafter, investigators were blinded to the group allocation. At sacrifice, blood was obtained via cardiac puncture, allowed to clot at room temperature, centrifuged at 4,000 g for 10 min. The serum was collected and then centrifuged at 4,000 g for 1 min. Urine was collected at study time points and flash frozen. The kidneys, liver, lung, heart, and muscle were collected at sacrifice; one-half of each was flash frozen, whereas the other one-half was formalin fixed and paraffin embedded. The heart was weighed and then separated by right and left ventricle (LV). The right ventricle and upper half of the LV were flash frozen. The caudal half of the LV was fixed in optimal cutting temperature (OCT) compound and then flash frozen. Weight was recorded at study time points. At sacrifice the tibia was dissected and length recorded, and the gastrocnemius muscle was dissected, flash frozen, and weighed.

KIDNEY FUNCTION. BUN and serum and urine creatinine were measured using a BioAssay Systems QuantiChrom Urea Assay Kit Cat: (DIUR-500) (BioAssay Systems, Hayward, California) and Pointe Scientific Creatinine (Enzymatic) Reagent Kit (Cat: C7548-480) (Pointe Scientific Inc, Canton, Michigan). Because of hemolysis, the 12-month SCr was determined using the Element DC Veterinary Chemistry Analyzer (Fujifilm, Serial # 73110474, Stamford, Connecticut [supported by Heska, Des Moines, Iowa]), using the Comparative Pathology Core at UC. Neutrophil gelatinase-associated lipocalin (NGAL) was measured by enzyme-linked immunosorbent assay (ELISA) (R and D Systems, Minneapolis, Minnesota), following the manufacturer's instructions (detection level: 8.8 pg/ml). Cytokines were measured by a customized U-Plex Biomarker-1 (Cat # K15069L-S, Meso Scale Discovery, Rockville, Maryland), following the manufacturer's instructions. Plasma renin was quantified using the Renin 1 Mouse ELISA Kit (Cat # EMREN1, Invitrogen, Carlsbad, California) and performed according to the manufacturer's instructions.

KIDNEY HISTOLOGY. Picrosirius red (PSR) was performed on kidney and standard histological staining procedures using Sirius Red F3B (Sigma-Aldrich, St. Louis, Missouri). Ten cortical images were visualized at 100× magnification using an Olympus BX41 microscope (Olympus, Waltham, Massachusetts) with a linear polarizer. Imaging software (Image J) was used to calculate the percent area of polarization. Immunohistochemistry for collagen type 3 was performed following standard protocols using goat anti-type III collagen antibody (Cat # 1330-01, Southern Biotech, Birmingham, Alabama [1:100]), followed by rabbit antigoat horseradish peroxidase (Ref # P0449, Dako,

FIGURE 2 Long-Term Kidney Sequelae in Mice After AKI

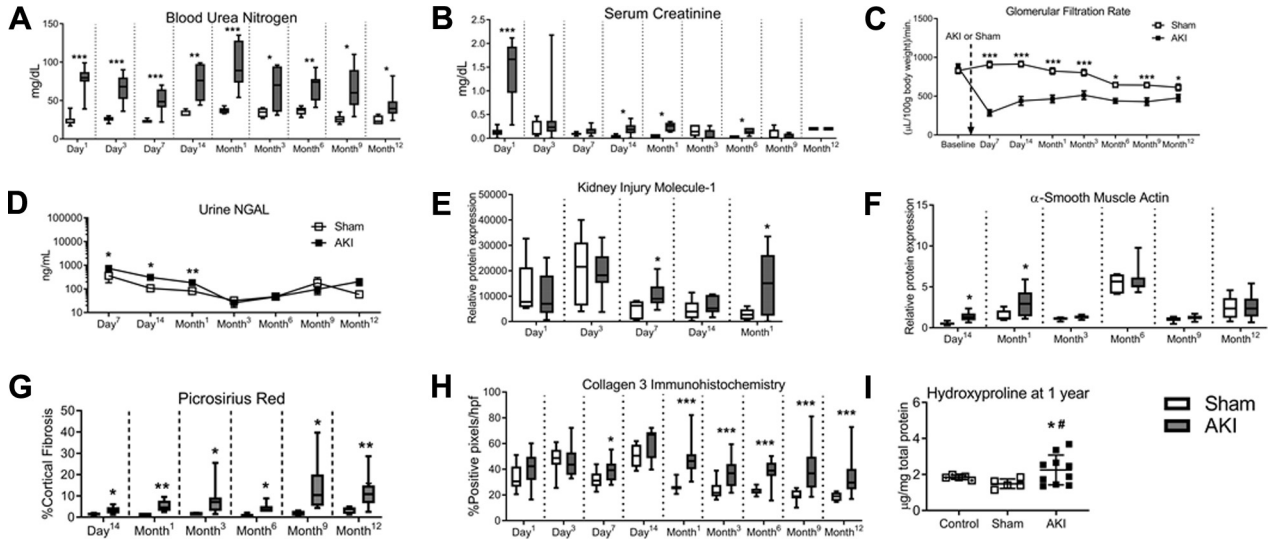

Male mice underwent 25 min of bilateral renal ischemia or sham procedure and were sacrificed 1, 3, 7, 14 days, or 1, 3, 6, 9, or 12 months later. **(A)** Blood urea nitrogen remained elevated after acute kidney injury (AKI) at all time points. **(B)** Serum creatinine improved and normalized after AKI. **(C)** Measured transcutaneous glomerular filtration rate, normalized for weight, remained decreased after AKI throughout the study. **(D)** Urine neutrophil gelatinase-associated lipocalin (NGAL) was elevated after AKI until1 month after the procedure. **(E)** AKI cohorts demonstrated an increase in protein expression for KIM-1 7 days and 1 month after AKI, and an increase in α-SMA at 14 days and 1 month **(F)**. **(G)** Quantification of kidney fibrosis via Picrosirius Red showed an increase in fibrosis in the AKI cohorts from day 14 throughout the 1 year study. **(H)** Quantification of immunohistochemistry in the kidneys for Collagen 3 showed an increase in the AKI cohorts at the day 7, and months 1, 3, 6, 9, and 12 time points. **(I)** Hydroxyproline content of the kidneys was assessed in the 12 month samples and showed an increase in the AKI cohort compared to both sham and unmanipulated age-matched controls (n = 5 to 11). *#p < 0.05 with AKI compared to sham or control, respectively. TGFR = transcutaneous glomerular filtration rate.

Carpinteria, California [1:200]) and analyzed as described previously (29). Both kidneys were analyzed for PSR and collagen 3, and the average was used for analysis.

WESTERN BLOT. Kidneys were homogenized and analyzed using 1× RIPA buffer (Cell Signaling Technology, Danvers, Massachusetts) with either α-smooth muscle actin (SMA) primary antibody (ab32575, Abcam, Cambridge, United Kingdom, 1:5000) or KIM-1 Primary antibody (Cat#: AF1817, R and D Systems, Minneapolis, Minnesota, 1:1000) as previously described (29). Blots were normalized using the Revert Total Protein Stain (Cat # 926-11010, Licor, Lincoln, Nebraska) as a loading control and performed following the manufacturer's instructions.

HYDROXYPROLINE ASSAY. Hydroxyproline content was measured in the left kidney from each sample, as previously reported (29).

ECHOCARDIOGRAPHY AND BLOOD PRESSURE. Transthoracic echocardiography and Doppler analyses using Vevo2100 instruments (VisualSonics, Toronto, Ontario, Canada), and mean arterial blood pressure measurements using a noninvasive computerized tail-cuff system (CODA High Throughput System, Kent Scientific Corp, Torrington, Connecticut) were performed as previously described (28).

LV COLLAGEN FRACTION. The percentage of collagen tissue in the LV was quantified on the 1-year cardiac tissue samples, as previously described (28).

CARDIAC ATP. Pre-weighed LV tissue was processed, using commercially available reagents as per the manufacturer's instructions (Abcam, ab833355) and were normalized to LV weight.

METABOLOMICS. Frozen heart and plasma samples were processed as previously reported (14). Mean values for each group were calculated, and Student's *t*-test was used for pairwise group comparisons. For single-molecule analysis, p values were adjusted for the false discovery rate (FDR), using Benjamini-Hochberg's ad hoc method (30). Statistical significance was set at $p < 0.05$. For pathway-enrichment analysis, metabolites with nominal p values < 0.05 were entered into the Pathway Analysis feature of

FIGURE 3 Cardiac Outcomes After AKI

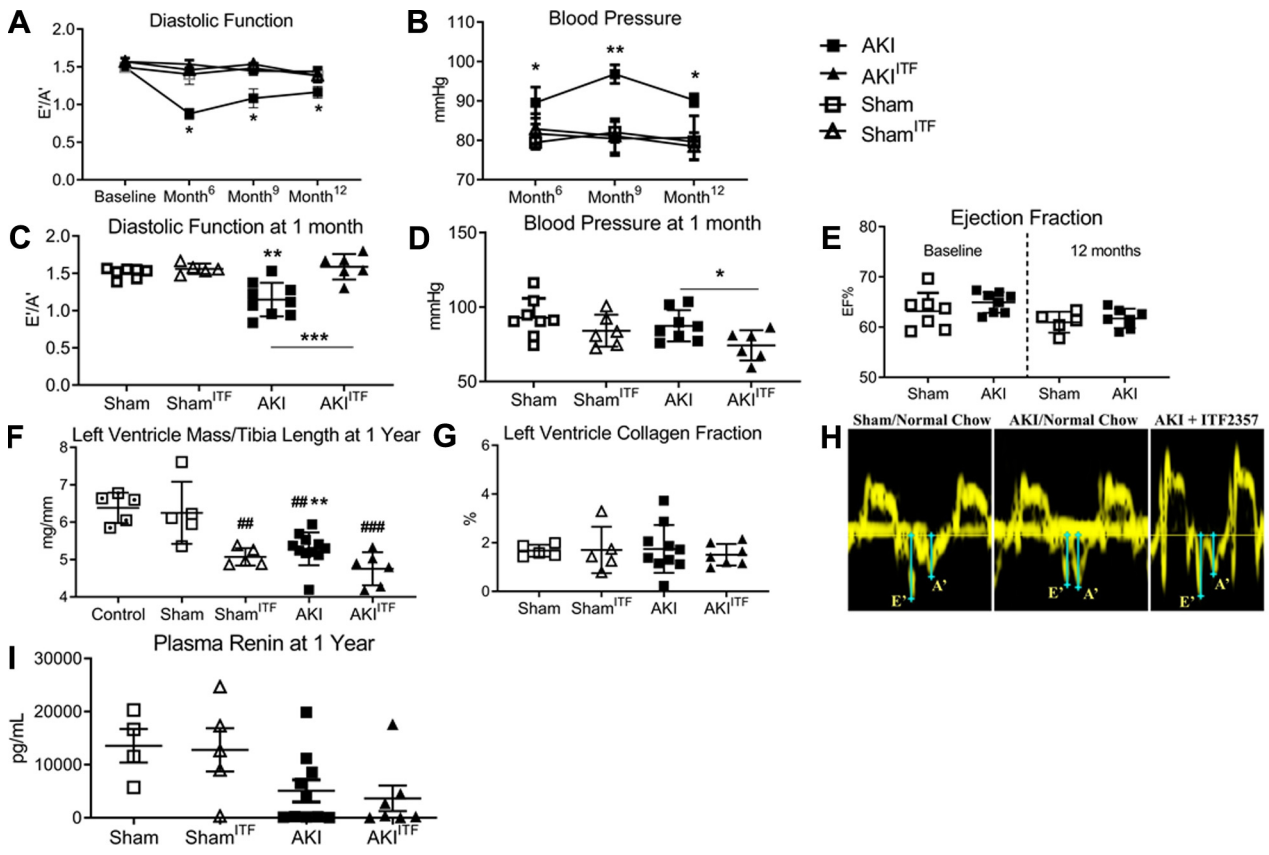

At 6, 9, and 12 months, AKI causes diastolic dysfunction (low E'/A') **(A)** and hypertension **(B)** but not in mice treated with ITF (AKI^{ITF}); At 1 month, AKI causes diastolic dysfunction **(C)** but not hypertension **(D)**, indicating that the diastolic dysfunction precedes the hypertension. One year after AKI, ejection fraction is preserved despite diastolic dysfunction and hypertension **(E)**. **(F)** AKI did not result in left ventricular hypertrophy nor increased collagen deposition **(G)** at 12 months. **(H)** Representative echocardiogram images 6 months after AKI or sham and treatment with ITF shows abnormal E' to A' ratio in the AKI cohort, and normalization in the AKI cohort treated with ITF2357. **(I)** Plasma renin levels 1 year after AKI or sham show no significant difference between groups (n = 5 to 11). *#p < 0.05 with AKI compared to sham or control, respectively. Abbreviation as in Figures 1 and 2.

MetaboAnalyst 3.0 (31). Compound Name was used to identify metabolites and was adjusted to comply with MetaboAnalyst limitations in nomenclature.

DETECTION OF LUNG MYELOPEROXIDASE. Lung myeloperoxidase (MPO) was measured as previously described (12).

STATISTICS. Comparisons among groups was performed via analysis of variance (ANOVA) with Tukey post hoc adjustment for multiple comparisons and p value <0.05 for significance. Comparison between 2 groups was performed using unpaired Student's *t*-tests, assuming Gaussian distribution with Welch's correction; p <0.05 for statistical significance. Data are presented as the mean ± standard error of the mean (SEM).

RESULTS

KIDNEY OUTCOMES. Cohorts contained n = 5 to 11. Mice were sacrificed after AKI or sham on post-operative days 1, 3, 7, 14 and months 1, 3, 6, 9, and 12 (Figure 1). BUN (Figure 2A) remained elevated throughout the 1-year study, whereas SCr (Figure 2B) recovered early but did not normalize until the 9-month time point. Serial kidney function was measured via tGFR; there was a diminishing but still significant reduction in tGFR 1 year after AKI (Figure 2C). Individual tGFR data for each time point are shown in Supplemental Figure 1. Figure 2D demonstrates an increase in urine NGAL in the AKI cohort up to 1 month, with no significant difference thereafter.

FIGURE 4 Long-Term Kidney Sequelae in Male Mice Treated With ITF2357

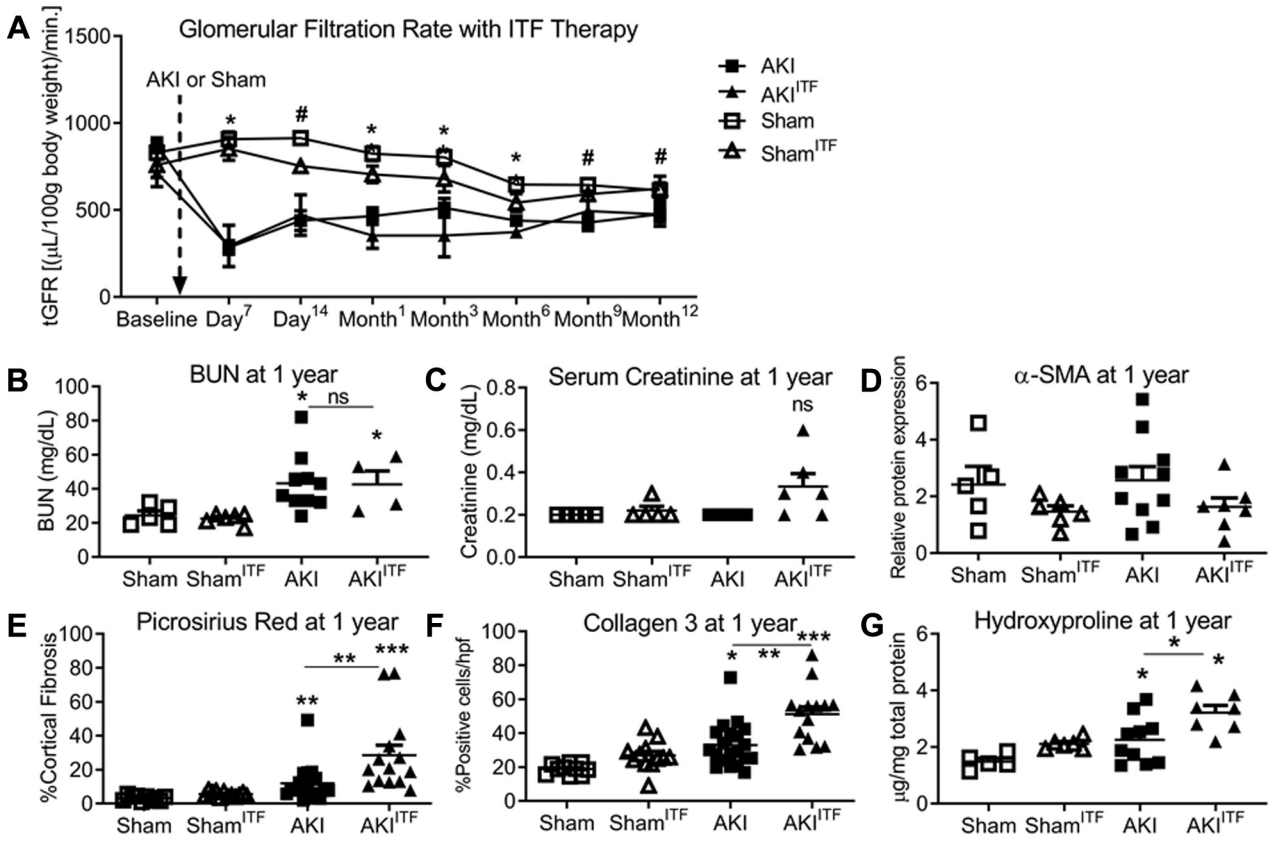

Long-term renal sequelae in male mice treated with ITF2357. Male mice underwent 25 min of bilateral renal ischemia or sham procedure, were started on chow containing ITF2357 3 days later, and were sacrificed 12 months later **(A).** Measured tGFR, normalized for weight, demonstrated no effect on measured tGFR throughout the year-long study between the AKI vs. AKI^{ITF} or Sham vs. Sham^{ITF} cohorts. **(B)** 12 months after AKI^{ITF}, blood urea nitrogen was elevated compared to sham^{ITF} while there was no significant difference between the AKI and AKI^{ITF} cohorts. There was no significant difference in measured serum creatinine **(C)** or α-SMA **(D)** amongst the 12 month groups. Quantification of fibrosis via Picrosirius Red **(E)**, Collagen 3 immunohistochemistry **(F)** and Hydroxyproline content **(G)** showed an increase in fibrosis markers at 12 months in the AKI^{ITF} cohorts compared to both sham^{ITF} and AKI cohorts. (n = 5 to 11) In **A**, * indicates a difference between both Sham vs. AKI and Sham^{ITF} vs. AKI^{ITF} * whereas # indicates there was only a difference between the Sham and AKI cohorts. Otherwise, * and # signify $p < 0.05$ with AKI compared to sham or control, respectively. Abbreviations as in Figure 1 and 2.

Western-blot analysis of kidney homogenates for kidney injury molecule-1 (KIM-1) (Figure 2E), and α-SMA (Figure 2F) showed an increase in the AKI cohorts compared with sham at 7 days and 1 month, and 14 days and 1 month, respectively.

Quantification of PSR staining (Figure 2G) and Collagen 3 immunohistochemistry (Figure 2H) demonstrated an increase in fibrosis markers in the AKI cohort, starting within 14 days and continuing throughout the study. Hydroxyproline content (Figure 2I) at 12 months was increased in the AKI cohort compared with both sham and unmanipulated controls. Cystic progression was also noted in the AKI cohorts, starting at the 3-month time point and continuing throughout the duration of the study.

EFFECT OF AKI AND HDACi ON CARDIAC OUTCOMES. Based on our previous work with ITF2357, we hypothesized that treatment would improve cardiac outcomes. Serial echocardiograms demonstrated diastolic dysfunction after AKI from 6 months onward; mice treated with ITF2357 did not develop diastolic dysfunction after AKI (Figure 3A). E'/A' represents the ratio of LV tissue velocity near the mitral valve during the first passive early filling phase (E') and second filling phase of atrial contraction (A'). The E'/A' ratio therefore represents a measure of LV

FIGURE 5 **Representative Picrosirius Red Staining 12 Months After AKI or Sham Procedure Without and With ITF2357 Treatment**

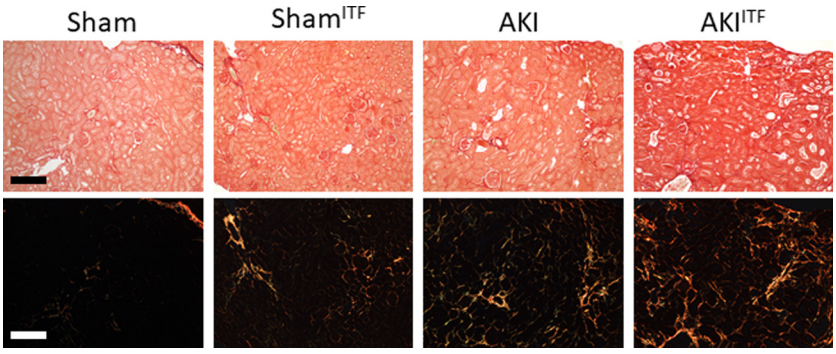

AKI results in increased fibrosis. ITF treatment did not improve kidney fibrosis. **(Top panels)** Light microscopy. **(Bottom panels)** Polarized images. Magnification, 100×. Scale bar = 10 μM. Abbreviation as in Figures 1 and 2.

relaxation, with a low ratio demonstrating slow wall velocities, indicating diastolic dysfunction. Mean arterial blood pressure measurements were obtained starting at 6 months and showed an increase in blood pressure in the AKI cohort at 6, 9, and 12 months; mice treated with ITF2357 did not develop hypertension after AKI (Figure 3B).

To determine whether the diastolic dysfunction was resulting from the hypertension or preceding it, we repeated the study of AKI with and without ITF2357 treatment and measured diastolic function and blood pressure 1 month after the AKI or sham procedure. Cohorts with AKI demonstrated diastolic dysfunction (Figure 3C) but not hypertension (Figure 3D), whereas those treated with ITF2357 developed neither.

Ejection fraction (EF) measures the percentage of blood that is ejected from the LV during systole. There were no significant differences of EF among the cohorts throughout the study period, and all groups maintained EF >60% post-procedure. Figure 3E shows that there was no difference in the baseline or 12-month EF between sham and AKI groups despite the diastolic dysfunction and hypertension found in the AKI groups; AKI was not causing heart failure with reduced EF. Figure 3H shows representative echocardiogram images of mice after sham (normal E'/A' ratio), AKI, (abnormal E'/A' ratio), and AKI^{ITF} (normal E'/A' ratio).

We next sought to determine whether left ventricular hypertrophy or cardiac fibrosis could explain the poor cardiac outcomes after AKI. Figure 3F shows the ratio of LV mass to tibia length, and Figure 3G shows the percent of collagen tissue in the left ventricle at 1 year; AKI did not result in either LV hypertrophy or increased collagen deposition.

To assess the contribution of the renin-angiotensin-aldosterone system on the development of hypertension, we measured plasma renin on the 12-month samples (Figure 3I). There was no significant difference in renin among the cohorts at the 12-month time point.

EFFECT OF HDACi ON KIDNEY OUTCOMES. One of the main purposes of this study was to investigate the cardiorenal effects of HDACi after AKI. We hypothesized that the improvement in cardiac outcomes after AKI in groups treated with ITF2357 may be secondary to improvement in renal outcomes: namely, mitigation of chronic kidney disease (CKD). We therefore sought to determine whether ITF2357 improved kidney function and histology. There was no difference in measured tGFR in the AKI^{ITF} cohort compared with the AKI group throughout the duration of the study. Measured tGFR demonstrated a significant reduction in kidney function in the AKI^{ITF} cohort compared with the sham^{ITF} cohort through the first 6 months (Figure 4A). At the 12-month time point, BUN was increased in the AKI^{ITF} group compared with sham^{ITF} (Figure 4B), but there was no statistically significant difference in SCr (Figure 4C). Treatment with ITF2357 did not affect α-SMA expression at the 1-year time point (Figure 4D). Urine NGAL was increased in the AKI^{ITF} cohort compared with sham^{ITF} at the 14-day, 1- and 12-month time points (Supplemental Figure 2A). Treatment with ITF2357 did not affect urine NGAL levels after AKI (Supplemental Figure 2B). Comparison of all 12-month study cohorts for PSR (Figure 4E), collagen 3 immunohistochemistry (Figure 4F), and hydroxyproline (Figure 4G) demonstrated an increase in fibrosis markers in the AKI^{ITF} relative to the sham^{ITF} and AKI groups.

FIGURE 6 AKI Affects Long-Term Body Composition

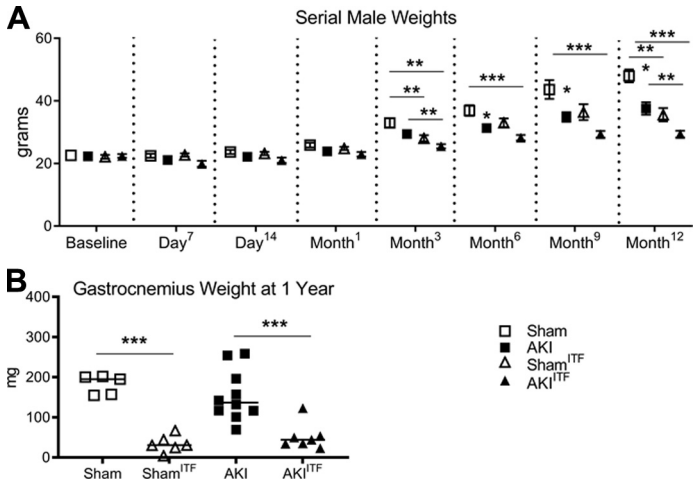

AKI affects long-term body composition. **(A)** Serial body weight measurements in the male cohorts demonstrate a widening reduction in body weight starting at 3 months post-procedure. AKI^{ITF} cohorts weighed the least by the end of the study. **(B)** Gastrocnemius weight after sacrifice 12 months after AKI or sham show reduced muscle weight in cohorts treated with ITF ($n = 5$ to 14). *$p < 0.05$ compared to sham control (AKI vs. sham, or AKI^{ITF} vs. sham^{ITF}). Abbreviations as in Figures 1 and 2.

Figure 5 shows representative PSR images. Taken in sum, ITF2357 had no effect on measures of kidney function and resulted in increased kidney fibrosis.

NONCARDIAC SYSTEMIC SEQUELAE. Having determined that the cardiac outcomes were not improved in the ITF2357 cohort via mitigation of CKD, we next investigated the noncardiorenal systemic outcomes to determine whether global organ protection or alterations in the metabolome explained the improvement in cardiac function and blood pressure. Figure 6A shows the serial weights of the cohorts over the course of the yearlong study. ITF2357 treatment was associated with a decrease in weight after both sham and AKI. The most significant difference in weight occurred between the sham and AKI^{ITF} cohorts, with the difference starting at month 3 and increasing throughout the duration of the study. By 6 months, there was also a significant reduction in weight in the AKI versus sham cohort, which increased throughout the rest of the study. Post hoc, we weighed the gastrocnemius muscle on the 12-month cohorts to assess the relative change in muscle mass with respect to AKI and ITF therapy. Figure 6B demonstrates that cohorts treated with ITF2357 had significant reductions in gastrocnemius mass 12 months after AKI or sham. There was no significant difference in measured muscle mass between the AKI and sham cohorts.

Lung MPO was measured to assess lung inflammation. Figure 7A demonstrates an increase in lung MPO in the AKI cohort compared with sham out to 14 days after injury with no difference thereafter and effect shown with ITF2357 treatment at the 1-year time point (Figure 7B). Serum ALT and aspartate aminotransferase (AST) were measured to screen for liver injury. Figure 8 demonstrates that ALT was increased in the AKI cohort 1 day after injury, with no significant difference in liver function tests at any other time point.

In the serial study, serum was measured for cytokines to assess for long-term immune system perturbations after AKI. Data for each cytokine can be found in Supplemental Figure 3. Several cytokines (IL-6, tumor necrosis factor [TNF]-α, IL-10, IL-4, IL-2, IL1β, CXCL1) demonstrated early increases after AKI, and most normalized within 1 to 2 weeks of injury. TNF-α demonstrated the most sustained elevations, with increased levels documented in the AKI cohort compared with sham 1 year after AKI.

EFFECT OF AKI AND HDACi ON METABOLISM. We performed metabolomics analysis on the 12-month cohorts to investigate whether the ITF2357 therapy affected cardiac outcomes via metabolic reprogramming. Although several individual molecules were significantly different between AKI and sham in both plasma and cardiac tissue (Supplemental Tables 1A and 1B), none met our criteria for significance by FDR. In cardiac tissue, metabolomics analysis (Supplemental Table 1A) demonstrated enrichment for several pathways involving amino acid metabolism. These included alanine, aspartate and glutamate metabolism (FDR <0.001); arginine and proline metabolism (FDR 0.002); valine, leucine, and isoleucine metabolism (FDR 0.030); and histidine metabolism (FDR 0.003). There was enrichment, particularly for amino acid pathways involving 1-carbon metabolism including cysteine and methionine metabolism (FDR <0.001); taurine and hypotaurine metabolism (FDR 0.010); glutathione metabolism (FDR 0.020); and glycine, serine, and threonine metabolism (FDR 0.040).

Finally, based on our findings of enrichment for energy-related pathways in plasma and the hypothesis that energy metabolism is disrupted in AKI, we analyzed key metabolites related to ATP metabolism. In heart tissue and plasma (Supplemental Figure 4) adenosine and adenosine monophosphate (AMP) (both precursors to ATP) were higher in AKI hearts without ITF2357. In both tissues, higher AMP and adenosine diphosphate (ADP) in the setting of lower ATP indicated less efficient energy metabolism. In

FIGURE 7 Lung Inflammation After AKI

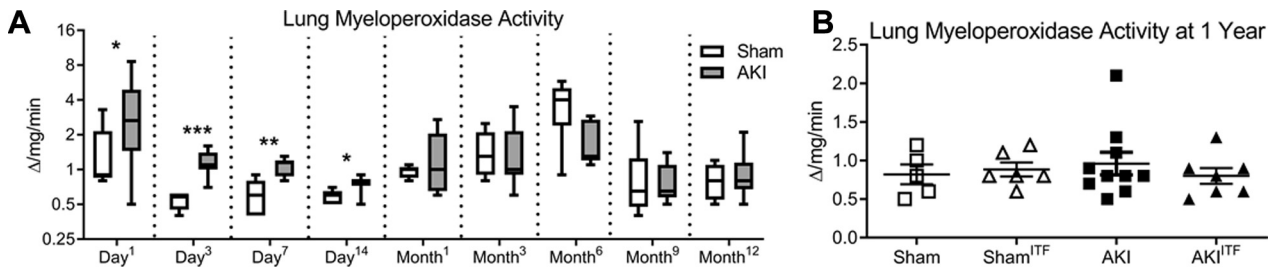

(A) Serial lung myeloperoxidase activity in the male acute kidney injury (AKI) versus sham cohorts demonstrates an increase in lung inflammation up to 14 days after kidney injury. **(B)** 1 year after AKI or sham procedure, there is no difference amongst cohorts with or without ITF2357 treatment (n = 5 to 14). *p < 0.05 compared to sham control.

heart tissue, this was despite a higher amount of diphosphate (p = 0.02) in the AKI hearts without ITF2357. Therefore, supply of phosphate in tissue cannot explain why AMP or adenosine was higher. Based on these cardiac metabolome findings, we hypothesized that levels of ATP would be reduced in mice after AKI, which would represent an energy deficit associated with AKI that is ameliorated with ITF2357 treatment. This is supported by other nonpurine molecules associated with energy use. Specifically, nicotinamide ribonucleotide (p = 0.010) was higher in the AKI group not treated with ITF2357 (Supplemental Figure 5). This is a precursor to nicotinamide adenine dinucleotide (NAD) that is converted to NAD via the enzyme encoded for by nicotinamide mononucleotide adenylyltransferase (NMNAT). When reduced to NADH by the tricarboxylic acid (TCA) cycle provides energy to the mitochondrial electron transport chain for 3 ATP molecules. Previous studies have found that low relative NAD formation is a key contributor to energy deficits in AKI (32). Here, although NAD+ is not different between AKI and AKI + ITF, the reaction ratio for NR to NAD+ via NMNAT (in AKI vs. AKI+ITF) favors the substrate (i.e., does not favor the forward reaction) in AKI (ratio 1.44; p = 0.29, NS). NADH was not able to be quantified in this assay. We next compared the effect of ITF2357 treatment on both the sham and AKI cohorts. When we examined pathways with shared enrichment in both AKI and sham with exposure to ITF2357 in cardiac tissue (Supplemental Table 2A), cysteine and methionine metabolism (FDR 0.001) was the primary pathway of enrichment. Metabolites that contributed to this enrichment (**Figure 9**) (33) include methionine, cysteine, glutathione, and S-adenosyl-homocysteine, which were all lower in the ITF-treated subjects (AKI^{ITF} and $sham^{ITF}$) versus those that did not receive ITF (AKI and sham). We then looked at pathways that were differentially enriched in either AKI or sham (not shared between the 2 groups) (Supplemental Table 3A) with exposure to ITF. Pathways enriched primarily included amino acid metabolism pathways involving alanine, aspartate, and glutamate metabolism (FDR 0.001), which is closely related to TCA cycle metabolism.

In plasma, metabolomics analysis (Supplemental Table 3B) demonstrated similar pathway enrichment to cardiac tissue. Evaluation of the effects of ITF on AKI and/or sham demonstrated enrichment for 1-carbon-related amino acid pathways including glycine, serine, and threonine metabolism (FDR 0.001); glutathione metabolism (FDR 0.010); and cysteine and methionine metabolism (FDR 0.047). Other amino acid pathways affected in ITF treatment included arginine and proline metabolism (FDR < 0.001); alanine, aspartate, and glutamate metabolism (FDR 0.020); and phenylalanine, tyrosine, and tryptophan metabolism (FDR 0.020). Interestingly, there was also enrichment for pathways involved in energy metabolism. These included the pentose phosphate pathway (FDR 0.001), purine metabolism (FDR 0.01), and glycolysis/gluconeogenesis (FDR 0.03).

As in cardiac tissue, we next analyzed shared versus differential effects of ITF2357 in AKI and sham in plasma (Supplemental Tables 2B and 3B, respectively). Shared effects of ITF2357 exposure in AKI and sham included pathway enrichment for 1-carbon amino acid- related pathways including glycine, serine, and threonine metabolism (FDR 0.010) and glutathione (FDR 0.047). The most significantly enriched pathway in plasma (Supplemental Figure 6)

FIGURE 8 Liver Function Tests After AKI

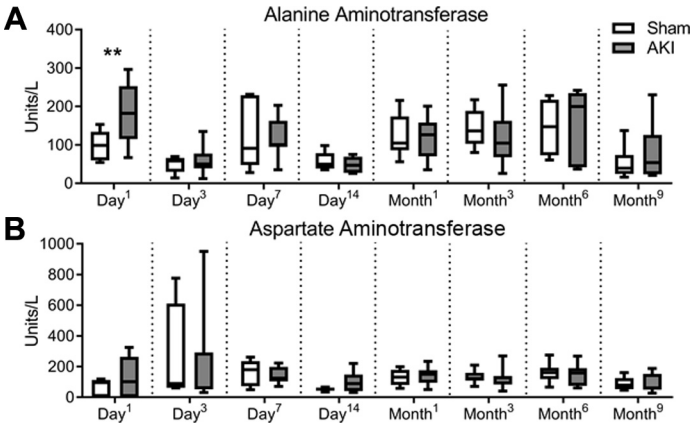

(A) The AKI cohort demonstrates an increase in alanine aminotransferase 1 day post-procedure but at no other time point. **(B)** There is no statistically significant difference between aspartate aminotransferase levels in AKI versus sham cohorts at any time point. *Nota bene*, measurements were unable to be obtained for the 12 month time point secondary to hemolysis (n = 5 to 13). *p < 0.05. Abbreviation as in Figure 1.

was arginine and proline metabolism (FDR < 0.001). Metabolites contributing to this enrichment include glutamine, arginine, guanidinoacetate (GAA), creatine, and creatinine involved in both nitrogen balance and energy metabolism. These were all higher in ITF-treated plasma (both AKI and sham groups). In plasma, pathways that were differentially enriched between AKI and sham with exposure to ITF (Supplemental Table 3B) included those related to energy metabolism, specifically purine metabolism (FDR 0.003) and the pentose phosphate pathway (FDR 0.030)

In summary, the metabolomics data suggest that AKI impairs energy utilization in the heart, specifically impairing the generation of ATP, and groups treated with ITF2357 demonstrated enhancement in pathways associated with 1-carbon metabolism.

EFFECT OF HDACi ON CARDIAC ATP LEVELS. Based on the metabolomics findings suggesting impairment in ATP generation after AKI, we next sought to determine whether persistently reduced levels of cardiac ATP could explain the diastolic dysfunction. ATP levels in cardiac tissue at 12 months showed significant reductions after AKI compared with sham; mice treated with ITF2357 had preservation of cardiac ATP levels (**Figure 10**). These results mirrored both our previously published short-term findings, and the long-term diastolic dysfunction after AKI in this study (14).

DISCUSSION

In this 1-year study, we have demonstrated the kidney and systemic consequences after a single episode of AKI in mice and evaluated the cardiorenal effects of HDAC inhibition.

Key findings of our study include the following:

1. AKI results in persistent diastolic dysfunction, which precedes the development of hypertension. EF was preserved, and there was no LV hypertrophy.
2. Treatment with HDACi prevents both diastolic dysfunction and hypertension after AKI and preserves cardiac levels of ATP.
3. Other systemic effects seen in the immediate aftermath of AKI, such as perturbances in serum IL-6 and lung inflammation, do not persist; however, there were significant differences in growth parameters after AKI, and these differences increased throughout the 1- year study.

We have previously demonstrated that AKI leads to diastolic dysfunction within 72 h (14), and this study demonstrates that these findings persist at 1, 3, 6, 9, and 12 months after AKI. These data suggest that systemic effects during the initial AKI episode are likely contributors to long-term cardiovascular disease and track with clinical data demonstrating that hospitalized patients with AKI have increased risks for developing heart failure or stroke after hospital discharge (19,22). In an observational study of US Veterans, Bansal et al. demonstrated a 23% increased risk for incident heart failure after AKI (34). In 1 of the most compelling studies to date, 1-year cardiovascular outcomes were assessed in 146,941 hospitalized adults, of whom 31,245 experienced AKI; after extensive adjustment for confounders, patients with AKI had a 44% increased rate of hospitalization for heart failure in the year following hospital discharge (22). Given these long-term effects, it has been hypothesized that the AKI episode is likely to initiate a persistent deleterious effect on cardiac function (20), which is consistent with the findings in the current study.

Treatment with HDACi mitigates these cardiac sequelae. It is possible that long-term effects on energy metabolism may be at play, as we previously identified ATP depletion in the heart at 24 h and 72 h after AKI (14), and ATP depletion was also present 1 year post-AKI. The cardiac and plasma metabolomics results indicate problems with energy metabolism: primarily impairment in generating ATP. We did not find a metabolic explanation for

FIGURE 9 Metabolomic Effects of ITF in AKI and/or Sham Heart Tissue at 1 Year

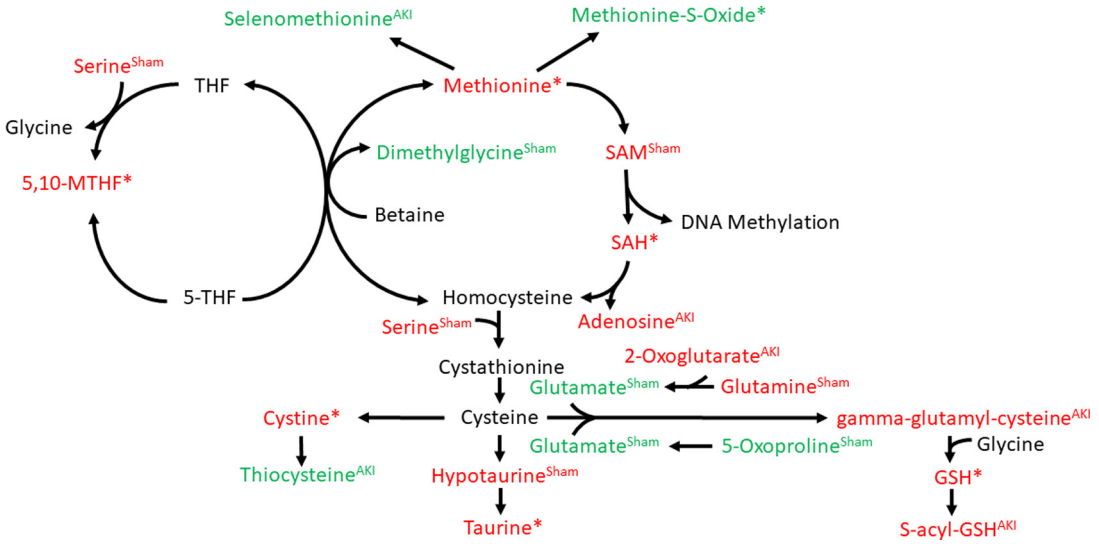

Pathway diagram illustrating the relative concentrations of one-carbon metabolites (i.e., cysteine and methionine pathway related metabolites) shared **(*)** or differentially between AKI and Sham cohorts, relative to ITF treatment in heart tissue. The pathway, enriched in metaboanalyst analysis, is adapted with permission from the Kyoto Encyclopedia of Genes and Genomes (KEGG) pathway 00270 (cysteine and methionine metabolism), 00480 (glutathione metabolism), and 00250 (alanine, aspartate, and glutamate metabolism). **Red** indicates lower concentrations in the ITF treated group, while **green** indicates higher concentrations. Abbreviations as in Figures 1 to 3.

the effect of AKI versus sham on long-term cardiac function; however, we did find significant differences in groups treated with HDACi. Namely, we found that groups treated with HDACi demonstrated improvement in multiple pathways involved in 1-carbon metabolism. One-carbon metabolism is central to methylation changes and epigenetic regulation across the genome, and it appears to be modified through ITF2357 exposure. Decreased ATP levels in the heart is a recognized cause of diastolic dysfunction (35). Thus, improved diastolic function in ITF2357 treated mice is likely caused, at least in part, by the ability of the HDACi to normalize cardiac ATP levels. Lkhagva et al. (36) have previously shown that Class I HDAC inhibition improves cardiomyocyte mitochondrial function and cardiac ATP levels after exposure to TNF-α. Our cytokine data demonstrate a persistent elevation in TNF-α in the AKI cohort compared with sham; however, there was no significant difference in TNF-α in the ITF2357 versus regular chow cohorts at the 12-month time point. Conversely, groups treated with ITF2357 had reduced plasma levels of CXCL1 at 1 year, which is consistent with previous reports (37), but there was no difference in CXCL1 in the AKI and sham cohorts without ITF treatment. In sum, the 1-year cytokine data suggest a cardioprotective mechanism of action beyond immunomodulation. The role of epigenetics and the potential therapeutic benefit of HDACi on cardiorenal outcomes remain under-investigated, and this is the first murine study to demonstrate long-term cardiac impairment after AKI (38–42).

We initiated HDACi treatment 3 days after the AKI or sham procedure to replicate a clinically feasible intervention time, as most AKI is diagnosed at least 48 h after the inciting event(s). The potential clinical implications of our cardiorenal findings would be profound if they are replicated in human studies. An important next step will be to investigate whether any such diastolic dysfunction is apparent in patients with AKI, with the recent report of diastolic dysfunction in elderly patients with AKI being notable (24).

Epidemiological studies in patients have demonstrated that patients with AKI are at increased risk of subsequent hypertension (43). AKI studies in rats have demonstrated impaired natriuresis after AKI, with resultant hypertension (44,45). As a result, it has been proposed that the development of hypertension

FIGURE 10 Treatment With HDACi Preserves Cardiac ATP Levels 1 Year After AKI

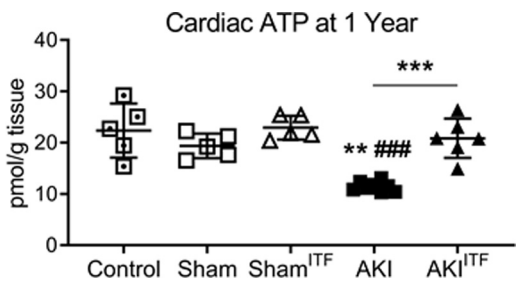

Treatment with Histone deacetylase inhibition (HDACi) preserves cardiac adenosine triphosphate (ATP) levels 1 year after AKI. At 12 months, AKI resulted in reduced levels of cardiac ATP and mice treated with ITF (AKI^{ITF}) had normal ATP levels ($n = 5$ to 11). *#$p < 0.05$ with AKI compared to sham or control, respectively. Abbreviations as in Figures 1 to 3.

following AKI has been intermediary step to developing heart failure. Our data in the current study suggest that hypertension is not a prerequisite for the development of diastolic dysfunction, as hypertension was absent in mice 1 month post-AKI, yet diastolic dysfunction was present. Whether subsequent hypertension is a maintenance factor for continued diastolic dysfunction is unknown. Yoon et al. showed Class I HDACi-treated hypertension in an obesity murine model via inhibition of angiotensin II (46). However, in our model, there was no significant difference in plasma renin levels at the 12-month time point, indicating that the renin-angiotensin-aldosterone system was not driving the hypertension in the AKI cohort. Others have shown that HDAC inhibition can mitigate hypertension in murine models of hypertension and that HDACi may result in vascular remodeling (47,48). Further studies are warranted to investigate the mechanism of development of hypertension following AKI.

It is notable that treatment with ITF2357 did not improve kidney outcomes in our study. Williams et al. (49) recently demonstrated mitigation of progression of chronic kidney disease with treatment of a pan-lysine deacetylase inhibitor in a murine model of glomerular disease. Further studies are needed to determine the potential benefits of various HDACi on murine models of disease and whether they elicit different cardiorenal effects.

Recently, the NIDDK published guidelines on overcoming the translational barriers in studying AKI and suggested that functional measurements as well as systemic sequelae be included in animal studies (50). In the longitudinal study, measured tGFR remained decreased, and there are increased markers of kidney fibrosis in the AKI cohorts 1 year after injury, despite early near-normalization of serum creatinine. These data support the limitations of serum creatinine as a clinically adequate biomarker of kidney function (51). Liu et al. (52) described the AKI-to-CKD transition in their 1-year murine model of bilateral renal ischemia (21 min) reperfusion injury and characterized the progression of cyst development, tubular atrophy, and fibrosis in male mice. This study focused on the long-term renal outcomes of AKI. Our histological results demonstrate similar findings with regard to fibrosis outcomes.

Our study is the first long-term investigation of the renal (including measured GFR) as well as systemic effects of AKI in mice. Our analysis of the plasma metabolome in the 12-month samples indicates that the subclinical CKD (kidney fibrosis and reduced tGFR with normal SCr) does not result in CKD-related perturbances to the circulating metabolome. Taken in sum with our previous publication evaluating earlier time points after AKI, the data suggest that the cardiac findings are a result of the AKI rather than any component of CKD.

Although the AKI mice appeared healthy after their initial recovery, their growth parameters were affected long term, with the AKI cohorts weighing significantly less than healthy and sham controls. Histone deacetylases play an important role in the pathogenesis of obesity, and the impact of HDACi on metabolism, insulin resistance, and thermogenic adipocyte differentiation varies depending on the class of HDACi (53–55). IFT2357 is a nonspecific HDACi that acts on Class I, IIa, IIb, and IV HDACs. In our model, groups treated with ITF2357 weighed less throughout the course of the study and had markedly reduced gastrocnemius mass, indicating a potential loss in lean-muscle mass. Further studies are needed to evaluate the impact of ITF2357 on body composition. Importantly, the impact of AKI in pediatric patients on their long-term growth parameters has not yet been described.

STUDY STRENGTHS AND LIMITATIONS. The strengths of our study include the numerous study time points, measurement of serial renal function (tGFR), and the HDACi treatment arm. The serial AKI versus sham study was robustly powered, although a limitation of the study was the use of fewer mice in the 12-month ITF2357 cohort. Another limitation was the significant hemolysis at the 12-month sacrifice of

the AKI and sham cohorts; this affected the methods by which we were able to measure SCr and made it impossible to measure ALT and AST. Although unfortunate, the preceding 6-month and 9-month data imply that the 12-month measurements would have been unlikely to demonstrate any significant findings with respect to liver enzymes. The study is strengthened by serial cardiorenal measurements, including tissue Doppler assessments of cardiac function; however, there are important limitations in assessing cardiac function, particularly after kidney injury (56). We endeavored to minimize any confounders in E' and A' assessment by using strict measurement criteria and only measured waveforms that were not merged, had complete separation, and did not have separation beyond the baseline. The study is further limited by lack of measurement of neurohormones other than renin that could affect control of blood pressure.

Future studies are needed to investigate the mechanism(s) by which HDACi improves cardiac outcomes following AKI. In a 5-week rat model, Basile et al. (57) demonstrated persistent oxidative stress following ischemia-reperfusion AKI. Others have demonstrated that oxidative stress causes epigenetic modifications in aging, as well as chronic diseases such as endometriosis and bone disease, and have shown the critical role of DNA methylation in cytosolic reactive oxygen species regulation (58–61). Coupled with previous findings on the impact of HDACi on cardiomyocyte mitochondrial function and ATP levels in a cardiomyocyte injury model (36), we hypothesize that AKI leads to sustained oxidative stress, resulting in impairment in energy utilization in cardiac mitochondria and that HDACi improves these outcomes via improvements in cardiomyocyte mitochondrial function that result in preservation of energy metabolism. Future studies are required to test this hypothesis.

Finally, this paper details the cardiorenal outcomes of male mice after AKI. Sex is an important biological variable, and estrogen is known to protect against ischemic AKI (62–65). Furthermore, energy metabolism and mitochondrial function are also affected by sex (66). Further investigations are needed to compare the cardiorenal and metabolomics outcomes of female mice after AKI.

CONCLUSIONS

In summary, we have demonstrated long-term diastolic dysfunction that precedes the development of hypertension and reduced levels of cardiac ATP 1 year after ischemia-reperfusion acute kidney injury in male mice. Treatment with ITF2357 prevents these cardiac sequelae but does not improve kidney function or histology.

FUNDING SUPPORT AND AUTHOR DISCLOSURES

Funding for this study was provided by the Consortium for Fibrosis Research & Translation (CFReT), supported through the University of Colorado School of Medicine's Transformational Research Funding initiative, and the National Institute of Diabetes and Digestive and Kidney Diseases (NIDDK) career development award program (DES, K08 DK109226-01A1). Dr. Montford has received support from the Veterans Health Administration (VHA) (IK2BX003839-02). Dr. McKinsey has received support from the National Institutes of Health (NIH) [HL147558, HL116848, HL127240, DK119594, and HL150225] and the American Heart Association [16FRN31400013]. Dr. Bagchi has received funding from the Canadian Institutes of Health Research (FRN-216927). Echocardiographic analysis was supported by National Institutes of Health grant 1S1-OD018156-01, entitled Small Animal Ultrasound Imager-Vevo 2100.

ADDRESS FOR CORRESPONDENCE: Dr. Danielle E. Soranno, University of Colorado, Department of Pediatrics, Pediatric Nephrology, 13123 East. 16th Avenue, Box 328 Aurora, Colorado 80045, USA. E-mail: Danielle.Soranno@childrenscolorado.org.

PERSPECTIVES

COMPETENCY IN MEDICAL KNOWLEDGE: Acute kidney injury is common in both pediatric and adult hospitalized patients. There is a growing appreciation that patients who develop AKI merit long-term nephrology follow-up. Our data add to growing epidemiological evidence that these patients may also merit closer cardiovascular surveillance. Furthermore, HDACi therapy may be of clinical benefit in mitigating long-term systemic sequelae after AKI; however, further studies are needed to investigate the mechanism of action as well as balancing measures such as the effect on growth and muscle.

TRANSLATIONAL OUTLOOK: Accumulating epidemiological data suggest the link between AKI and later cardiovascular disease; however, the pathophysiology is not yet known. Herein, our animal model demonstrates a direct link between AKI and persistent diastolic dysfunction. Our data show that a clinically available therapeutic histone deacetylase inhibitor, ITF2357, initiated at the clinically feasible time point of 3 days after injury, serves as a potential novel treatment to improve cardiovascular outcomes. Future research is needed to determine whether our findings translate clinically.

REFERENCES

1. Kaddourah A, Basu RK, Bagshaw SM, Goldstein SL, AWARE Investigators. Epidemiology of acute kidney injury in critically ill children and young adults. N Engl J Med 2017;376:11–20.

2. Hoste EAJ, Kellum JA, Selby NM, et al. Global epidemiology and outcomes of acute kidney injury. Nat Rev Nephrol 2018;14:607–25.

3. Hobson C, Ozrazgat-Balsanti T, Kuxhausen A, et al. Cost and mortality associated with postoperative acute kidney injury. Ann Surg 2015;261:1207–14.

4. Jurawan N, Pankurst T, Ferro C, et al. Hospital acquired acute kidney injury is associated with increased mortality but not increased readmission rates in a UK acute hospital. BMC Nephrol 2017;18:317.

5. Chertow GM, Burdick E, Honour M, Bonventre JV, Bates DW. Acute kidney injury, mortality, length of stay, and costs in hospitalized patients. J Am Soc Nephrol 2005;16:3365–70.

6. Silver SA, Long J, Zheng Y, Chertow GM. Cost of acute kidney injury in hospitalized patients. J Hosp Med 2017;12:70–6.

7. Searns JB, Gist KM, Brinton JT, et al. Impact of acute kidney injury and nephrotoxic exposure on hospital length of stay. Pediatr Nephrol 2020;35:799–806.

8. Selby NM, Kolhe NV, McIntyre CW, et al. Defining the cause of death in hospitalised patients with acute kidney injury. PLoS One 2012;7:e48580.

9. Mehta RL, Pascual MT, Soroko S, et al. Spectrum of acute renal failure in the intensive care unit: the PICARD experience. Kidney Int 2004;66:1613–21.

10. Faubel S. Acute kidney injury and multiple organ dysfunction syndrome. Minerva Urol Nefrol 2009;61:171–88.

11. Klein CL, Hoke JS, Fang W-F, Altmann CJ, Douglas IS, Faubel S. Interleukin-6 mediates lung injury following ischemic acute kidney injury or bilateral nephrectomy. Kidney Int 2008;74:901–9.

12. Andres-Hernando A, Altmann C, Bhargava R, et al. Prolonged acute kidney injury exacerbates lung inflammation at 7 days post-acute kidney injury. Physiol Rep 2014;2.

13. Ahuja N, Andres-Hernando A, Altmann C, et al. Circulating IL-6 mediates lung injury via CXCL1 production after acute kidney injury in mice. Am J Physiol Renal Physiol 2012;303:F864–72.

14. Fox BM, Gil H-W, Kirkbride-Romero L, et al. Metabolomics assessment reveals oxidative stress and altered energy production in the heart after ischemic acute kidney injury in mice. Kidney Int 2019;95:590–610.

15. Kelly KJ. Distant effects of experimental renal ischemia/reperfusion injury. J Am Soc Nephrol 2003;14:1549–58.

16. Sumida M, Doi K, Ogasawara E, et al. Regulation of mitochondrial dynamics by dynamin-related protein-1 in acute cardiorenal syndrome. J Am Soc Nephrol 2015;26:2378–87.

17. Chawla LS. Acute kidney injury leading to chronic kidney disease and long-term outcomes of acute kidney injury: the best opportunity to mitigate acute kidney injury? Contrib Nephrol 2011;174:182–90.

18. Chawla LS, Eggers PW, Starr RA, Kimmel PL. Acute kidney injury and chronic kidney disease as interconnected syndromes. N Engl J Med 2014;371:58–66.

19. Gammelager H, Christiansen CE, Johanssen MB, Tønnessen E, Jespersen B, Sørensen HT. Three-year risk of cardiovascular disease among intensive care patients with acute kidney injury: a population-based cohort study. Crit Care 2014;18:492.

20. Chawla LS, Amdur RL, Shaw AD, Faselis C, Palant CE, Kimmel PL. Association between AKI and long-term renal and cardiovascular outcomes in United States veterans. Clin J Am Soc Nephrol 2013;9:448–56.

21. Wu VC, Wu C-H, Huang T-M, et al. Long-term risk of coronary events after AKI. J Am Soc Nephrol 2014;25:595–605.

22. Go AS, Hsu C-Y, Yang J, et al. Acute kidney injury and risk of heart failure and atherosclerotic events. Clin J Am Soc Nephrol 2018;13:833–41.

23. James M, Bouchard J, Ho J, et al. Canadian Society of Nephrology commentary on the 2012 KDIGO clinical practice guideline for acute kidney injury. Am J Kidney Dis 2013;61:673–85.

24. Cho W, Hwang TY, Choi YK, et al. Diastolic dysfunction and acute kidney injury in elderly patients with femoral neck fracture. Kidney Res Clin Pract 2019;38:33–41.

25. Li W, Sun Z. Mechanism of action for HDAC inhibitors: insights from omics approaches. Int J Mol Sci 2019;20:1616.

26. Bush EW, McKinsey TA. Protein acetylation in the cardiorenal axis: the promise of histone deacetylase inhibitors. Circ Res 2010;106:272–84.

27. Myasoedova VA, Grechko AV, Zhang D, Orekhov AN. Inhibitors of DNA methylation and histone deacetylation as epigenetically active drugs for anticancer therapy. Curr Pharm Des 2019;25:635–41.

28. Jeong MY, Lin YH, Wennersten SA, et al. Histone deacetylase activity governs diastolic dysfunction through a nongenomic mechanism. Sci Transl Med 2018;10.

29. Soranno DE, Gil HW, Kirkbride-Romero L, et al. Matching human unilateral AKI, a reverse translational approach to investigate kidney recovery after ischemia. J Am Soc Nephrol 2019;30:990–1005.

30. Hochberg Y, Benjamini Y. More powerful procedures for multiple significance testing. Stat Med 1990;9:811–8.

31. Xia J, Sinelnikov IV, Han B, Wishort DS. MetaboAnalyst 3.0: making metabolomics more meaningful. Nucleic Acids Res 2015;43:W251–7.

32. Mehr AP, Tran MT, Ralto KM, et al. De novo NAD(+) biosynthetic impairment in acute kidney injury in humans. Nat Med 2018;24:1351.

33. Kanehisa M, Goto S. KEGG: kyoto encyclopedia of genes and genomes. Nucleic Acids Res 2000;28:27–30.

34. Bansal N, Matheny ME, Greevy RA Jr., et al. Acute kidney injury and risk of incident heart failure among US veterans. Am J Kidney Dis 2018;71:236–45.

35. Periasamy M, Janssen PM. Molecular basis of diastolic dysfunction. Heart Fail Clin 2008;4:13–21.

36. Lkhagva B, Kao YH, Lee TI, Lee TW, Cheng WL, Chen YJ. Activation of class I histone deacetylases contributes to mitochondrial dysfunction in cardiomyocytes with altered complex activities. Epigenetics 2018;13:376–85.

37. Gonneaud A, Gagné JM, Turgeon N, Asselin C. The histone deacetylase Hdac1 regulates inflammatory signalling in intestinal epithelial cells. J Inflamm (Lond) 2014;11:43.

38. Bagshaw SM, Hoste EA, Braam B, et al. Cardiorenal syndrome type 3: pathophysiologic and epidemiologic considerations. Contrib Nephrol 2013;182:137–57.

39. Cruz DN, Gheorghiade M, Palazzuoli A, Ronco C, Bagshaw SM. Epidemiology and outcome of the cardio-renal syndrome. Heart Fail Rev 2011;16:531–42.

40. Goh CY, Virzi G, De Cal M, Ronco C. Cardiorenal syndrome: a complex series of combined heart/kidney disorders. Contrib Nephrol 2011;174:33–45.

41. Rosner MH, Rastogi A, Ronco C. The cardiorenal syndrome. Int J Nephrol 2011;2011:982092.

42. Virzi GM, Clementi A, Brocca A, de Cal M, Ronco C. Epigenetics: a potential key mechanism involved in the pathogenesis of cardiorenal syndromes. J Nephrol 2018;31:333–41.

43. Hsu CY, Hsu RK, Yang J, Ordonez JD, Zheng S, Go AS. Elevated BP after AKI. J Am Soc Nephrol 2016;27:914–23.

44. Spurgeon-Pechman KR, Donohoe DL, Mattson DL, Lund H, James L. Recovery from acute renal failure predisposes hypertension and secondary renal disease in response to elevated sodium. Am J Physiol Renal Physiol 2007;293:F269–78.

45. Pechman KR, De Miguel C, Lund H, Basile DP, Mattson DL. Recovery from renal ischemia-reperfusion injury is associated with altered renal hemodynamics, blunted pressure natriuresis, and sodium-sensitive hypertension. Am J Physiol Regul Integr Comp Physiol 2009;297:R1358–63.

46. Yoon GE, Jung JK, Lee YH, Jang BC, Kim J. Histone deacetylase inhibitor CG200745 ameliorates high-fat diet-induced hypertension via inhibition of angiotensin II production. Naunyn Schmiedebergs Arch Pharmacol 2020;393:491–500.

47. Iyer A, Fenning A, Lim J, et al. Antifibrotic activity of an inhibitor of histone deacetylases in DOCA-salt hypertensive rats. Br J Pharmacol 2010;159:1408–17.

48. Cardinale JP, Sriramula S, Pariaut R, et al. HDAC inhibition attenuates inflammatory, hypertrophic, and hypertensive responses in spontaneously hypertensive rats. Hypertension 2010;56:437–44.

49. Williams VR, Konvalinka A, Song X, et al. Connectivity mapping of a chronic kidney disease progression signature identified lysine deacetylases as novel therapeutic targets. Kidney Int 2020;98:116–32.

50. Zuk A, Palevsky PM, Fried L, et al. Overcoming translational barriers in acute kidney injury: a report from an NIDDK workshop. Clin J Am Soc Nephrol 2018;13:1113–23.

51. Lopez-Giacoman S, Madero M. Biomarkers in chronic kidney disease, from kidney function to kidney damage. World J Nephrol 2015;4:57–73.

52. Liu J, Kumar S, Dolzhenko E, et al. Molecular characterization of the transition from acute to chronic kidney injury following ischemia/reperfusion. JCI Insight 2017;2:e94716.

53. Ong BX, Brunmeir R, Zhang Q, et al. Regulation of thermogenic adipocyte differentiation and adaptive thermogenesis through histone acetylation. Front Endocrinol (Lausanne) 2020;11:95.

54. Ferrari A, Fiorino E, Longo R, et al. Attenuation of diet-induced obesity and induction of white fat browning with a chemical inhibitor of histone deacetylases. Int J Obes (Lond) 2017;41:289–98.

55. Priya Nijhawan TB, Khullar G, Pal G, Kandhwal M, Goyal A. HDAC in obesity: a critical insight. Obes Med 2020;18:100212.

56. Nagueh SF, Smithseth OA, Appleton CP, et al. Recommendations for the evaluation of left ventricular diastolic function by echocardiography: an update from the American Society of Echocardiography and the European Association of Cardiovascular Imaging. Eur Heart J Cardiovasc Imaging 2016;7:1321–60.

57. Basile DP, Leonard EC, Beal AG, Schleuter D, Friedrich J. Persistent oxidative stress following renal ischemia-reperfusion injury increases ANG II hemodynamic and fibrotic activity. Am J Physiol Renal Physiol 2012;302:F1494–502.

58. Ito F, Yamada Y, Shigemitsu A, et al. Role of oxidative stress in epigenetic modification in endometriosis. Reprod Sci 2017;24:1493–502.

59. Vrtacnik P, Zupan J, Mlakar V, et al. Epigenetic enzymes influenced by oxidative stress and hypoxia mimetic in osteoblasts are differentially expressed in patients with osteoporosis and osteoarthritis. Sci Rep 2018;8:16215.

60. Guillaumet-Adkins A, Yañez Y, Peris-Diaz MD, Calabria I, Palanca-Ballester C, Sandoval J. Epigenetics and oxidative stress in aging. Oxid Med Cell Longev 2017;2017:9175806.

61. Duraisamy AJ, Mishra M, Kowluru A, Kowluru RA. Epigenetics and regulation of oxidative stress in diabetic retinopathy. Invest Ophthalmol Vis Sci 2018;59:4831–40.

62. Lee SK. Sex as an important biological variable in biomedical research. BMB Rep 2018;51:167–73.

63. Miller LR, Marks C, Becker JB, et al. Considering sex as a biological variable in preclinical research. FASEB J 2017;31:29–34.

64. Takaoka M, Yuba M, Fujii T, Ohkita M, Matsumara Y. Oestrogen protects against ischaemic acute renal failure in rats by suppressing renal endothelin-1 overproduction. Clin Sci (Lond) 2002;103 Suppl 48:434S–7S.

65. Satake A, Takaoka M, Nishikawa M, et al. Protective effect of 17beta-estradiol on ischemic acute renal failure through the PI3K/Akt/eNOS pathway. Kidney Int 2008;73:308–17.

66. Cardinale DA, Larsen FJ, Schiffer TA, et al. Superior intrinsic mitochondrial respiration in women than in men. Front Physiol 2018;9:1133.

KEY WORDS acute kidney injury, cardiorenal syndrome, diastolic dysfunction, histone deacetylase inhibition, systemic sequelae of kidney disease

APPENDIX For supplemental figures and tables, please see the online version of this paper.